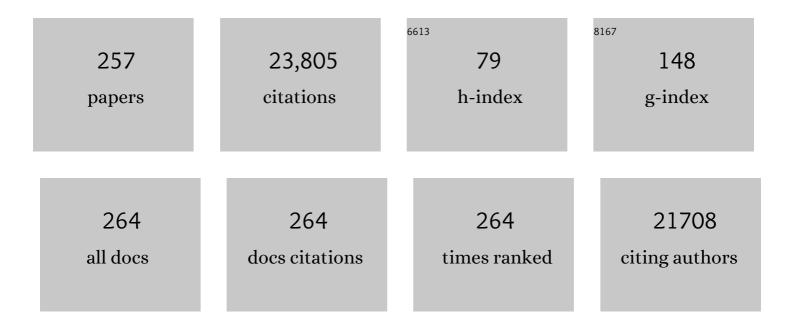
Geoff J M Parker

List of Publications by Year in descending order

Source: https://exaly.com/author-pdf/8586130/publications.pdf Version: 2024-02-01



#	Article	IF	CITATIONS
1	A tractometry principal component analysis of white matter tract network structure and relationships with cognitive function in relapsing-remitting multiple sclerosis. NeuroImage: Clinical, 2022, 34, 102995.	2.7	1
2	Bias, Repeatability and Reproducibility of Liver <scp>T₁</scp> Mapping With Variable Flip Angles. Journal of Magnetic Resonance Imaging, 2022, 56, 1042-1052.	3.4	7
3	Evaluation of Dynamic <scp>Contrastâ€Enhanced MRI</scp> Measures of Lung Congestion and Endothelial Permeability in Heart Failure: A Prospective Method Validation Study. Journal of Magnetic Resonance Imaging, 2022, , .	3.4	1
4	Quantitative kinetic modelling and mapping of cerebral glucose transport and metabolism using glucoCESL MRI. Journal of Cerebral Blood Flow and Metabolism, 2022, 42, 2066-2079.	4.3	1
5	Electrospinning for healthcare: recent advancements. Journal of Materials Chemistry B, 2021, 9, 939-951.	5.8	81
6	Innovations and advances in electrospraying technology. , 2021, , 207-228.		0
7	Image Contrast, Image Pre-Processing, and T1 Mapping Affect MRI Radiomic Feature Repeatability in Patients with Colorectal Cancer Liver Metastases. Cancers, 2021, 13, 240.	3.7	12
8	Dynamic contrast-enhanced MRI of synovitis in knee osteoarthritis: repeatability, discrimination and sensitivity to change in a prospective experimental study. European Radiology, 2021, 31, 5746-5758.	4.5	12
9	Optimization of quantitative susceptibility mapping for regional estimation of oxygen extraction fraction in the brain. Magnetic Resonance in Medicine, 2021, 86, 1314-1329.	3.0	5
10	Alzheimer's disease pathology is associated with earlier alterations to blood–brain barrier water permeability compared with healthy ageing in TgF344â€AD rats. NMR in Biomedicine, 2021, 34, e4510.	2.8	20
11	Effect of oxaliplatin plus 5-fluorouracil or capecitabine on circulating and imaging biomarkers in patients with metastatic colorectal cancer: a prospective biomarker study. BMC Cancer, 2021, 21, 354.	2.6	1
12	A model selection framework to quantify microvascular liver function in gadoxetateâ€enhanced MRI: Application to healthy liver, diseased tissue, and hepatocellular carcinoma. Magnetic Resonance in Medicine, 2021, 86, 1829-1844.	3.0	4
13	Sources of systematic error in DCEâ€MRI estimation of lowâ€level bloodâ€brain barrier leakage. Magnetic Resonance in Medicine, 2021, 86, 1888-1903.	3.0	21
14	Validating pore size estimates in a complex microfiber environment on a human MRI system. Magnetic Resonance in Medicine, 2021, 86, 1514-1530.	3.0	5
15	Coaxial electrospun biomimetic copolymer fibres for application in diffusion magnetic resonance imaging. Bioinspiration and Biomimetics, 2021, 16, 046016.	2.9	4
16	Comparative analysis of signal models for microscopic fractional anisotropy estimation using q-space trajectory encoding. NeuroImage, 2021, 242, 118445.	4.2	6
17	Mechanisms of Network Changes in Cognitive Impairment in Multiple Sclerosis. Neurology, 2021, 97, e1886-e1897.	1.1	18
18	Characterisation of microvessel blood velocity and segment length in the brain using multi-diffusion-time diffusion-weighted MRI. Journal of Cerebral Blood Flow and Metabolism, 2021, 41, 0271678X2097852.	4.3	3

#	Article	IF	CITATIONS
19	Quantitative Magnetic Resonance Imaging in Perianal Crohn's Disease at 1.5 and 3.0 T: A Feasibility Study. Diagnostics, 2021, 11, 2135.	2.6	2
20	Extracellular resistance is sensitive to tissue sodium status; implications for bioimpedance-derived fluid volume parameters in chronic kidney disease. Journal of Nephrology, 2020, 33, 119-127.	2.0	13
21	Measuring water exchange across the blood-brain barrier using MRI. Progress in Nuclear Magnetic Resonance Spectroscopy, 2020, 116, 19-39.	7.5	49
22	The challenges of deploying artificial intelligence models in a rapidly evolving pandemic. Nature Machine Intelligence, 2020, 2, 298-300.	16.0	45
23	A tutorial and tool for exploring feature similarity gradients with MRI data. NeuroImage, 2020, 221, 117140.	4.2	26
24	Diffusion model comparison identifies distinct tumor subâ€regions and tracks treatment response. Magnetic Resonance in Medicine, 2020, 84, 1250-1263.	3.0	6
25	A structural connectivity convergence zone in the ventral and anterior temporal lobes: Data-driven evidence from structural imaging. Cortex, 2019, 120, 298-307.	2.4	26
26	Reproducing Fingerprints: A Step toward Clinical Adoption. Radiology, 2019, 292, 438-439.	7.3	0
27	Multidimensional diffusion MRI with spectrally modulated gradients reveals unprecedented microstructural detail. Scientific Reports, 2019, 9, 9026.	3.3	58
28	Salt and Water Retention Is Associated with Microinflammation and Endothelial Injury in Chronic Kidney Disease. Nephron, 2019, 143, 234-242.	1.8	17
29	Towards a â€~resolution limit' for DWâ€MRI tumor microstructural models: A simulation study investigating the feasibility of distinguishing between microstructural changes. Magnetic Resonance in Medicine, 2019, 81, 2288-2301.	3.0	10
30	Oxygen-enhanced MRI Is Feasible, Repeatable, and Detects Radiotherapy-induced Change in Hypoxia in Xenograft Models and in Patients with Non–small Cell Lung Cancer. Clinical Cancer Research, 2019, 25, 3818-3829.	7.0	51
31	Co-electrospraying of tumour cell mimicking hollow polymeric microspheres for diffusion magnetic resonance imaging. Materials Science and Engineering C, 2019, 101, 217-227.	7.3	11
32	Measuring tissue sodium concentration: Crossâ€vendor repeatability and reproducibility of ²³ Naâ€MRI across two sites. Journal of Magnetic Resonance Imaging, 2019, 50, 1278-1284.	3.4	17
33	Water-exchange MRI detects subtle blood-brain barrier breakdown in Alzheimer's disease rats. NeuroImage, 2019, 184, 349-358.	4.2	52
34	Mapping whole brain connectivity changes: The potential impact of different surgical resection approaches for temporal lobe epilepsy. Cortex, 2019, 113, 1-14.	2.4	8
35	Final results of the phase 1/2, open-label clinical study of intravenous recombinant human N-acetyl-1±-d-glucosaminidase (SBC-103) in children with mucopolysaccharidosis IIIB. Molecular Genetics and Metabolism, 2019, 126, 131-138.	1.1	17
36	Volumetric dynamic oxygen-enhanced MRI (OE-MRI): comparison with CT Brody score and lung function in cystic fibrosis patients. European Radiology, 2018, 28, 4037-4047.	4.5	20

#	Article	IF	CITATIONS
37	A biomimetic tumor tissue phantom for validating diffusionâ€weighted MRI measurements. Magnetic Resonance in Medicine, 2018, 80, 147-158.	3.0	12
38	Axon mimicking hydrophilic hollow polycaprolactone microfibres for diffusion magnetic resonance imaging. Materials and Design, 2018, 137, 394-403.	7.0	14
39	Assessing Inflammation in Acute Intracerebral Hemorrhage with PK11195 PET and Dynamic Contrast-Enhanced MRI. , 2018, 28, 158-161.		15
40	Dataâ€driven mapping of hypoxiaâ€related tumor heterogeneity using DCEâ€MRI and OEâ€MRI. Magnetic Resonance in Medicine, 2018, 79, 2236-2245.	3.0	18
41	Evaluation of dynamic contrast-enhanced MRI biomarkers for stratified cancer medicine: How do permeability and perfusion vary between human tumours?. Magnetic Resonance Imaging, 2018, 46, 98-105.	1.8	20
42	Plasma Tie2 is a tumor vascular response biomarker for VEGF inhibitors in metastatic colorectal cancer. Nature Communications, 2018, 9, 4672.	12.8	47
43	Delivering Functional Imaging on the MRI-Linac: Current Challenges and Potential Solutions. Clinical Oncology, 2018, 30, 702-710.	1.4	39
44	Microstructural imaging of the human brain with a â€~super-scanner': 10 key advantages of ultra-strong gradients for diffusion MRI. NeuroImage, 2018, 182, 8-38.	4.2	138
45	OC-0632: Oxygen enhanced-MRI is feasible, repeatable and detects radiotherapy-induced NSCLC hypoxia changes. Radiotherapy and Oncology, 2018, 127, S336-S337.	0.6	2
46	Stability and reproducibility of co-electrospun brain-mimicking phantoms for quality assurance of diffusion MRI sequences. NeuroImage, 2018, 181, 395-402.	4.2	9
47	Mapping Hypoxia in Renal Carcinoma with Oxygen-enhanced MRI: Comparison with Intrinsic Susceptibility MRI and Pathology. Radiology, 2018, 288, 739-747.	7.3	34
48	AB1186â€Dynamic contrast enhanced mr imaging in early stage knee osteoarthritis: a test-retest repeatability study in healthy and moderately diseased subjects. , 2018, , .		0
49	Early experience of oxygen enhanced magnetic resonance imaging (OE-MRI) in ataxia telangiectasia (A-T). , 2018, , .		0
50	The tract terminations in the temporal lobe: Their location and associated functions. Cortex, 2017, 97, 277-290.	2.4	48
51	Repeatability and response to therapy of dynamic contrast-enhanced magnetic resonance imaging biomarkers in rheumatoid arthritis in a large multicentre trial setting. European Radiology, 2017, 27, 3662-3668.	4.5	20
52	A graded tractographic parcellation of the temporal lobe. NeuroImage, 2017, 155, 503-512.	4.2	55
53	Hollow Polycaprolactone Microspheres with/without a Single Surface Hole by Co-Electrospraying. Langmuir, 2017, 33, 13262-13271.	3.5	28
54	Imaging biomarker roadmap for cancer studies. Nature Reviews Clinical Oncology, 2017, 14, 169-186.	27.6	792

#	Article	lF	CITATIONS
55	SAT0624â€Quantitative 3D imaging of tenosynovitis and bone marrow edema by DCE-MRI is a sensitive measure of response to therapy in rheumatoid arthritis. , 2017, , .		0
56	Oxygen Enhanced Optoacoustic Tomography (OE-OT) Reveals Vascular Dynamics in Murine Models of Prostate Cancer. Theranostics, 2017, 7, 2900-2913.	10.0	83
57	Inter-tumor validation, through advanced MRI and circulating biomarkers, of plasma Tie2 as the vascular response biomarker for bevacizumab Journal of Clinical Oncology, 2017, 35, 11521-11521.	1.6	0
58	Evaluation of non-contrast MRI biomarkers in lupus nephritis. Clinical and Experimental Rheumatology, 2017, 35, 954-958.	0.8	4
59	Biomimetic phantom for cardiac diffusion MRI. Journal of Magnetic Resonance Imaging, 2016, 43, spcone-spcone.	3.4	1
60	Biomimetic phantom for cardiac diffusion MRI. Journal of Magnetic Resonance Imaging, 2016, 43, 594-600.	3.4	24
61	Preparation and characterization of polycaprolactone microspheres by electrospraying. Aerosol Science and Technology, 2016, 50, 1201-1215.	3.1	29
62	COPD Patients Have Short Lung Magnetic ResonanceT1Relaxation Time. COPD: Journal of Chronic Obstructive Pulmonary Disease, 2016, 13, 153-159.	1.6	17
63	Mitotic Activity in Glioblastoma Correlates with Estimated Extravascular Extracellular Space Derived from Dynamic Contrast-Enhanced MR Imaging. American Journal of Neuroradiology, 2016, 37, 811-817.	2.4	23
64	Oxygen-Enhanced MRI Accurately Identifies, Quantifies, and Maps Tumor Hypoxia in Preclinical Cancer Models. Cancer Research, 2016, 76, 787-795.	0.9	133
65	T1-weighted Dynamic Contrast-enhanced MR Imaging of the Lung in Asthma: Semiquantitative Analysis for the Assessment of Contrast Agent Kinetic Characteristics. Radiology, 2016, 278, 906-916.	7.3	8
66	T1 Relaxation Time in Lungs of Asymptomatic Smokers. PLoS ONE, 2016, 11, e0149760.	2.5	8
67	Respiratory tract exacerbations revisited: Ventilation, inflammation, perfusion, and structure (VIPS) monitoring to redefine treatment. Pediatric Pulmonology, 2015, 50, S57-65.	2.0	29
68	Validation of High-Resolution Tractography Against <i>In Vivo</i> Tracing in the Macaque Visual Cortex. Cerebral Cortex, 2015, 25, 4299-4309.	2.9	101
69	Mixedâ€effects modeling of clinical DCEâ€MRI data: Application to colorectal liver metastases treated with bevacizumab. Journal of Magnetic Resonance Imaging, 2015, 41, 132-141.	3.4	9
70	SAT0601â€A Novel, Fully 3-Dimensional Dynamic Contrast MRI Method in the Hand Reveals Details of Synovial Inflammation and Provides a Sensitive Measure of Change. Annals of the Rheumatic Diseases, 2015, 74, 879.1-879.	0.9	0
71	Biomimetic phantom for the validation of diffusion magnetic resonance imaging. Magnetic Resonance in Medicine, 2015, 73, 299-305.	3.0	57
72	P284â€V/Q scanning using oxygen-enhanced Magnetic Resonance Imaging. Thorax, 2015, 70, A221-A221.	5.6	0

#	Article	IF	CITATIONS
73	Co-electrospun Brain Mimetic Hollow Microfibres Fibres for Diffusion Magnetic Resonance Imaging. Nanoscience and Technology, 2015, , 289-304.	1.5	2
74	MR Quantitative Equilibrium Signal Mapping: A Reliable Alternative to CT in the Assessment of Emphysema in Patients with Chronic Obstructive Pulmonary Disease. Radiology, 2015, 275, 579-588.	7.3	12
75	Production and cross-sectional characterization of aligned co-electrospun hollow microfibrous bulk assemblies. Materials Characterization, 2015, 109, 25-35.	4.4	24
76	Dynamic oxygen-enhanced magnetic resonance imaging of the lung in asthma—Initial experience. European Journal of Radiology, 2015, 84, 318-326.	2.6	39
77	The grey matter correlates of impaired decision-making in multiple sclerosis. Journal of Neurology, Neurosurgery and Psychiatry, 2015, 86, 530-536.	1.9	30
78	Imaging Intratumor Heterogeneity: Role in Therapy Response, Resistance, and Clinical Outcome. Clinical Cancer Research, 2015, 21, 249-257.	7.0	497
79	Ground Truth for Diffusion MRI in Cancer: A Model-Based Investigation of a Novel Tissue-Mimetic Material. Lecture Notes in Computer Science, 2015, 24, 179-190.	1.3	6
80	Dynamic Contrast-Enhanced Magnetic Resonance Imaging. , 2015, , 1-5.		0
81	Dynamic Contrast-Enhanced Magnetic Resonance Imaging. , 2015, , 1439-1443.		0
82	Secondary Progressive and Relapsing Remitting Multiple Sclerosis Leads to Motor-Related Decreased Anatomical Connectivity. PLoS ONE, 2014, 9, e95540.	2.5	17
83	Measurement of the Curie temperature distribution in FePt granular magnetic media. Applied Physics Letters, 2014, 104, .	3.3	41
84	Diffusion tensor MRI phantom exhibits anomalous diffusion. , 2014, 2014, 746-9.		9
85	Mutual information as a measure of image quality for 3D dynamic lung imaging with EIT. Physiological Measurement, 2014, 35, 863-879.	2.1	23
86	Validation of Tractography. , 2014, , 453-480.		4
87	MRI diffusion tractography study in individuals with schizotypal features: A pilot study. Psychiatry Research - Neuroimaging, 2014, 221, 49-57.	1.8	9
88	Noninvasive tumor hypoxia measurement using magnetic resonance imaging in murine U87 glioma xenografts and in patients with glioblastoma. Magnetic Resonance in Medicine, 2014, 71, 1854-1862.	3.0	54
89	Voxel-wise quantification of myocardial blood flow with cardiovascular magnetic resonance: effect of variations in methodology and validation with positron emission tomography. Journal of Cardiovascular Magnetic Resonance, 2014, 16, 11.	3.3	31
90	Multiparametric cardiovascular magnetic resonance surveillance of acute cardiac allograft rejection and characterisation of transplantation-associated myocardial injury. Journal of Cardiovascular Magnetic Resonance, 2014, 16, P394.	3.3	1

#	Article	IF	CITATIONS
91	Voxel-wise quantification of myocardial blood flow with cardiovascular magnetic resonance: effect of variations in methodology and validation with positron emission tomography. Journal of Cardiovascular Magnetic Resonance, 2014, 16, P352.	3.3	0
92	Multiparametric cardiovascular magnetic resonance assessment of cardiac allograft vasculopathy. Journal of Cardiovascular Magnetic Resonance, 2014, 16, O3.	3.3	0
93	Feasibility assessment of using oxygen-enhanced magnetic resonance imaging for evaluating the effect of pharmacological treatment in COPD. European Journal of Radiology, 2014, 83, 2093-2101.	2.6	30
94	Multiparametric cardiovascular magnetic resonance surveillance of acute cardiac allograft rejection and characterisation of transplantation-associated myocardial injury: a pilot study. Journal of Cardiovascular Magnetic Resonance, 2014, 16, 52.	3.3	51
95	Multiparametric Cardiovascular Magnetic Resonance Assessment of Cardiac Allograft Vasculopathy. Journal of the American College of Cardiology, 2014, 63, 799-808.	2.8	82
96	Indexed distribution analysis for improved significance testing of spatially heterogeneous parameter maps: Application to dynamic contrastâ€enhanced MRI biomarkers. Magnetic Resonance in Medicine, 2014, 71, 1299-1311.	3.0	6
97	Brain tissue modifications induced by cholinergic therapy in Alzheimer's disease. Human Brain Mapping, 2013, 34, 3158-3167.	3.6	14
98	The CONNECT project: Combining macro- and micro-structure. NeuroImage, 2013, 80, 273-282.	4.2	121
99	A phase 1 trial of intravenous 4-(N-(S-glutathionylacetyl)amino) phenylarsenoxide (CSAO) in patients with advanced solid tumours. Cancer Chemotherapy and Pharmacology, 2013, 72, 1343-1352.	2.3	33
100	Comprehensive Validation of Cardiovascular Magnetic Resonance Techniques for the Assessment of Myocardial Extracellular Volume. Circulation: Cardiovascular Imaging, 2013, 6, 373-383.	2.6	324
101	Anatomical brain connectivity can assess cognitive dysfunction in multiple sclerosis. Multiple Sclerosis Journal, 2013, 19, 1161-1168.	3.0	33
102	Using in vivo probabilistic tractography to reveal two segregated dorsal †language-cognitive' pathways in the human brain. Brain and Language, 2013, 127, 230-240.	1.6	25
103	Response to Letter Regarding Article, "Comprehensive Validation of Cardiovascular Magnetic Resonance Techniques for the Assessment of Myocardial Extracellular Volume― Circulation: Cardiovascular Imaging, 2013, 6, e26-7.	2.6	4
104	Diffusion MRI-based cortical complexity alterations associated with executive function in multiple sclerosis. Journal of Magnetic Resonance Imaging, 2013, 38, 54-63.	3.4	17
105	Effects of grain microstructure on magnetic properties in FePtAg-C media for heat assisted magnetic recording. Journal of Applied Physics, 2013, 113, .	2.5	31
106	<i>R</i> ₁ and <i>R</i> ₂ * changes in the human placenta in response to maternal oxygen challenge. Magnetic Resonance in Medicine, 2013, 70, 1427-1433.	3.0	68
107	083 HISTOLOGICAL VALIDATION OF DYNAMIC-EQUILIBRIUM CARDIOVASCULAR MAGNETIC RESONANCE FOR THE ASSESSMENT OF MYOCARDIAL EXTRACELLULAR VOLUME. Heart, 2013, 99, A51-A52.	2.9	0
108	084 EFFECT OF CONTRAST DOSE, POST-CONTRAST ACQUISITION TIME, MYOCARDIAL REGIONALITY, CARDIAC CYCLE AND GENDER ON DYNAMIC-EQUILIBRIUM CONTRAST CMR MEASUREMENT OF MYOCARDIAL EXTRACELLULAR VOLUME. Heart, 2013, 99, A52.1-A52.	2.9	0

#	Article	IF	CITATIONS
109	Mutual information as a measure of reconstruction quality in 3D dynamic lung EIT. Journal of Physics: Conference Series, 2013, 434, 012082.	0.4	0
110	DCE-MRI: acquisition and analysis techniques. , 2013, , 58-74.		15
111	Convergent Connectivity and Graded Specialization in the Rostral Human Temporal Lobe as Revealed by Diffusion-Weighted Imaging Probabilistic Tractography. Journal of Cognitive Neuroscience, 2012, 24, 1998-2014.	2.3	194
112	Coaxially Electrospun Axon-Mimicking Fibers for Diffusion Magnetic Resonance Imaging. ACS Applied Materials & Interfaces, 2012, 4, 6311-6316.	8.0	34
113	Dynamic contrast-enhanced MRI in clinical trials of antivascular therapies. Nature Reviews Clinical Oncology, 2012, 9, 167-177.	27.6	318
114	The variation of function across the human insula mirrors its patterns of structural connectivity: Evidence from in vivo probabilistic tractography. NeuroImage, 2012, 59, 3514-3521.	4.2	183
115	Fusion of images obtained from EIT and MRI. Electronics Letters, 2012, 48, 617.	1.0	9
116	Groupâ€averaged anatomical connectivity mapping for improved human white matter pathway visualisation. NMR in Biomedicine, 2012, 25, 1224-1233.	2.8	19
117	Imaging vascular function for early stage clinical trials using dynamic contrast-enhanced magnetic resonance imaging. European Radiology, 2012, 22, 1451-1464.	4.5	138
118	DCEâ€MRI model selection for investigating disruption of microvascular function in livers with metastatic disease. Journal of Magnetic Resonance Imaging, 2012, 35, 196-203.	3.4	25
119	Axon diameter mapping in the presence of orientation dispersion with diffusion MRI. NeuroImage, 2011, 56, 1301-1315.	4.2	240
120	Anatomical connectivity mapping: A new tool to assess brain disconnection in Alzheimer's disease. NeuroImage, 2011, 54, 2045-2051.	4.2	73
121	A two-part Phase II study of cediranib in patients with advanced solid tumours: the effect of food on single-dose pharmacokinetics and an evaluation of safety, efficacy and imaging pharmacodynamics. Cancer Chemotherapy and Pharmacology, 2011, 68, 631-641.	2.3	22
122	The effect of blood inflow and <i>B</i> ₁ â€field inhomogeneity on measurement of the arterial input function in axial 3D spoiled gradient echo dynamic contrastâ€enhanced MRI. Magnetic Resonance in Medicine, 2011, 65, 108-119.	3.0	61
123	Comparison of dynamic contrastâ€enhanced MRI and dynamic contrastâ€enhanced CT biomarkers in bladder cancer. Magnetic Resonance in Medicine, 2011, 66, 219-226.	3.0	20
124	Jet deposition in near-field electrospinning of patterned polycaprolactone and sugar-polycaprolactone core–shell fibres. Polymer, 2011, 52, 3603-3610.	3.8	68
125	Structural and optical properties of different dielectric thin films for planar waveguiding applications. , 2011, , .		1
126	Brain Hemispheric Structural Efficiency and Interconnectivity Rightward Asymmetry in Human and Nonhuman Primates. Cerebral Cortex, 2011, 21, 56-67.	2.9	171

#	Article	IF	CITATIONS
127	DCE-MRI biomarkers of tumour heterogeneity predict CRC liver metastasis shrinkage following bevacizumab and FOLFOX-6. British Journal of Cancer, 2011, 105, 139-145.	6.4	123
128	Dynamic Contrast-Enhanced Magnetic Resonance Imaging. , 2011, , 1173-1176.		0
129	The inferior, anterior temporal lobes and semantic memory clarified: Novel evidence from distortion-corrected fMRI. Neuropsychologia, 2010, 48, 1689-1696.	1.6	159
130	Distortion correction for diffusionâ€weighted MRI tractography and fMRI in the temporal lobes. Human Brain Mapping, 2010, 31, 1570-1587.	3.6	139
131	Multipleâ€bolus dynamic contrastâ€enhanced MRI in the pancreas during a glucose challenge. Journal of Magnetic Resonance Imaging, 2010, 32, 622-628.	3.4	11
132	Tracer kinetic analysis of dynamic contrastâ€enhanced MRI and CT bladder cancer data: A preliminary comparison to assess the magnitude of water exchange effects. Magnetic Resonance in Medicine, 2010, 64, 595-603.	3.0	35
133	Measurement of arterial plasma oxygenation in dynamic oxygenâ€enhanced MRI. Magnetic Resonance in Medicine, 2010, 64, 1838-1842.	3.0	16
134	Investigating Regional Pulmonary Compliance In Chronic Obstructive Pulmonary Disease And Healthy Volunteers Using Novel Proton MRI Method. , 2010, , .		0
135	The Ventral and Inferolateral Aspects of the Anterior Temporal Lobe Are Crucial in Semantic Memory: Evidence from a Novel Direct Comparison of Distortion-Corrected fMRI, rTMS, and Semantic Dementia. Cerebral Cortex, 2010, 20, 2728-2738.	2.9	378
136	Identification of early predictive imaging biomarkers and their relationship to serological angiogenic markers in patients with ovarian cancer with residual disease following cytotoxic therapy. Annals of Oncology, 2010, 21, 1982-1989.	1.2	27
137	Candidate Biomarkers of Extravascular Extracellular Space: A Direct Comparison of Apparent Diffusion Coefficient and Dynamic Contrast-Enhanced MR Imaging—Derived Measurement of the Volume of the Extravascular Extracellular Space in Glioblastoma Multiforme. American Journal of Neuroradiology, 2010, 31, 549-553.	2.4	61
138	Enhancing Fraction in Glioma and Its Relationship to the Tumoral Vascular Microenvironment: A Dynamic Contrast-Enhanced MR Imaging Study. American Journal of Neuroradiology, 2010, 31, 726-731.	2.4	26
139	Orientationally invariant indices of axon diameter and density from diffusion MRI. NeuroImage, 2010, 52, 1374-1389.	4.2	629
140	Imaging angiogenesis of genitourinary tumors. Nature Reviews Urology, 2010, 7, 69-82.	3.8	27
141	Probabilistic Fiber Tracking. , 2010, , 396-408.		6
142	Cross-Visit Tumor Sub-segmentation and Registration with Outlier Rejection for Dynamic Contrast-Enhanced MRI Time Series Data. Lecture Notes in Computer Science, 2010, 13, 121-128.	1.3	4
143	Selective inhibition of proliferating endothelial cells: A phase I study of the novel organoarsenical compound GSAO in patients with advanced solid tumors Journal of Clinical Oncology, 2010, 28, TPS167-TPS167.	1.6	0
144	Quantifying Antivascular Effects of Monoclonal Antibodies to Vascular Endothelial Growth Factor: Insights from Imaging. Clinical Cancer Research, 2009, 15, 6674-6682.	7.0	142

#	Article	IF	CITATIONS
145	Defining Meyer's loop-temporal lobe resections, visual field deficits and diffusion tensor tractography. Brain, 2009, 132, 1656-1668.	7.6	158
146	Using the Model-Based Residual Bootstrap to Quantify Uncertainty in Fiber Orientations From \$Q\$-Ball Analysis. IEEE Transactions on Medical Imaging, 2009, 28, 535-550.	8.9	42
147	Modeling of contrast agent kinetics in the lung using <i>T</i> ₁ â€weighted dynamic contrastâ€enhanced MRI. Magnetic Resonance in Medicine, 2009, 61, 1507-1514.	3.0	58
148	Comparison of normal tissue <i>R</i> _{<i>1</i>} and <i>R</i> modulation by oxygen and carbogen. Magnetic Resonance in Medicine, 2009, 61, 75-83.	3.0	77
149	Comparison of modelâ€based arterial input functions for dynamic contrastâ€enhanced MRI in tumor bearing rats. Magnetic Resonance in Medicine, 2009, 61, 1173-1184.	3.0	84
150	Quantifying spatial heterogeneity in dynamic contrastâ€enhanced MRI parameter maps. Magnetic Resonance in Medicine, 2009, 62, 488-499.	3.0	123
151	Preliminary Study of Oxygen-Enhanced Longitudinal Relaxation in MRI: A Potential Novel Biomarker of Oxygenation Changes in Solid Tumors. International Journal of Radiation Oncology Biology Physics, 2009, 75, 1209-1215.	0.8	107
152	Tumour enhancing fraction (EnF) in glioma: relationship to tumour grade. European Radiology, 2009, 19, 1489-1498.	4.5	16
153	Validation of Tractography. , 2009, , 353-375.		13
154	Oxygen-induced changes in longitudinal relaxation times in skeletal muscle. Magnetic Resonance Imaging, 2008, 26, 221-227.	1.8	24
155	Distortion correction for a double inversion-recovery sequence with an echo-planar imaging readout. Magnetic Resonance Imaging, 2008, 26, 943-953.	1.8	3
156	Evidence for Segregated and Integrative Connectivity Patterns in the Human Basal Ganglia. Journal of Neuroscience, 2008, 28, 7143-7152.	3.6	695
157	White matter tracts in first-episode psychosis: A DTI tractography study of the uncinate fasciculus. NeuroImage, 2008, 39, 949-955.	4.2	114
158	Tractography of the parahippocampal gyrus and material specific memory impairment in unilateral temporal lobe epilepsy. NeuroImage, 2008, 40, 1755-1764.	4.2	86
159	Probabilistic fibre tracking: Differentiation of connections from chance events. NeuroImage, 2008, 42, 1329-1339.	4.2	103
160	Quantitative imaging biomarkers in the clinical development of targeted therapeutics: current and future perspectives. Lancet Oncology, The, 2008, 9, 766-776.	10.7	150
161	White matter connections reflect changes in voluntary-guided saccades in pre-symptomatic Huntington's disease. Brain, 2008, 131, 196-204.	7.6	153
162	Combined EEG-fMRI and tractography to visualise propagation of epileptic activity. Journal of Neurology, Neurosurgery and Psychiatry, 2008, 79, 594-597.	1.9	61

#	Article	IF	CITATIONS
163	Imaging language pathways predicts postoperative naming deficits. Journal of Neurology, Neurosurgery and Psychiatry, 2008, 79, 327-330.	1.9	62
164	Glandular Function in Sjögren Syndrome: Assessment with Dynamic Contrast-enhanced MR Imaging and Tracer Kinetic Modeling—Initial Experience. Radiology, 2008, 246, 845-853.	7.3	27
165	Regularized super-resolution for diffusion MRI. , 2008, , .		9
166	A non-linear registration method for DCE-MRI and DCE-CT comparison in bladder tumors. , 2008, , .		4
167	Pharmacodynamic assessment of the anti-angiogenic and anti-vascular properties of bevacizumab by magnetic resonance imaging in metastatic colorectal carcinoma (CRC). Journal of Clinical Oncology, 2008, 26, 3546-3546.	1.6	0
168	Dynamic Contrast-Enhanced Magnetic Resonance Imaging. , 2008, , 920-923.		0
169	Enhancing Fraction Predicts Clinical Outcome following First-Line Chemotherapy in Patients with Epithelial Ovarian Carcinoma. Clinical Cancer Research, 2007, 13, 6130-6135.	7.0	23
170	Exploiting peak anisotropy for tracking through complex structures. , 2007, , .		31
171	Imaging Tumor Vascular Heterogeneity and Angiogenesis using Dynamic Contrast-Enhanced Magnetic Resonance Imaging. Clinical Cancer Research, 2007, 13, 3449-3459.	7.0	293
172	Phase I Evaluation of a Fully Human Anti–αv Integrin Monoclonal Antibody (CNTO 95) in Patients with Advanced Solid Tumors. Clinical Cancer Research, 2007, 13, 2128-2135.	7.0	136
173	Phase I Evaluation of CDP791, a PEGylated Di-Fab′ Conjugate that Binds Vascular Endothelial Growth Factor Receptor 2. Clinical Cancer Research, 2007, 13, 7113-7118.	7.0	69
174	Abnormal brain connectivity in first-episode psychosis: A diffusion MRI tractography study of the corpus callosum. NeuroImage, 2007, 35, 458-466.	4.2	111
175	Abnormalities of language networks in temporal lobe epilepsy. NeuroImage, 2007, 36, 209-221.	4.2	157
176	Diffusion tensor MRI-based estimation of the influence of brain tissue anisotropy on the effects of transcranial magnetic stimulation. NeuroImage, 2007, 36, 1159-1170.	4.2	102
177	Validation of in vitro probabilistic tractography. NeuroImage, 2007, 37, 1267-1277.	4.2	212
178	DCE-MRI biomarkers in the clinical evaluation of antiangiogenic and vascular disrupting agents. British Journal of Cancer, 2007, 96, 189-195.	6.4	467
179	What levels of precision are achievable for quantification of perfusion and capillary permeability surface area product using ASL?. Magnetic Resonance in Medicine, 2007, 58, 281-289.	3.0	34
180	Organâ€specific effects of oxygen and carbogen gas inhalation on tissue longitudinal relaxation times. Magnetic Resonance in Medicine, 2007, 58, 490-496.	3.0	75

#	Article	IF	CITATIONS
181	Tracer kinetic model–driven registration for dynamic contrastâ€enhanced MRI timeâ€series data. Magnetic Resonance in Medicine, 2007, 58, 1010-1019.	3.0	71
182	Quantifying Heterogeneity in Dynamic Contrast-Enhanced MRI Parameter Maps. , 2007, 10, 376-384.		11
183	Comparison of the Performance of Tracer Kinetic Model-Driven Registration for Dynamic Contrast Enhanced MRI Using Different Models of Contrast Enhancement. Academic Radiology, 2006, 13, 1112-1123.	2.5	43
184	Hemispheric asymmetries in language-related pathways: A combined functional MRI and tractography study. NeuroImage, 2006, 32, 388-399.	4.2	373
185	In vivo diffusion tensor imaging of the human optic nerve: Pilot study in normal controls. Magnetic Resonance in Medicine, 2006, 56, 446-451.	3.0	74
186	Comparison of errors associated with single- and multi-bolus injection protocols in low-temporal-resolution dynamic contrast-enhanced tracer kinetic analysis. Magnetic Resonance in Medicine, 2006, 56, 611-619.	3.0	32
187	Experimentally-derived functional form for a population-averaged high-temporal-resolution arterial input function for dynamic contrast-enhanced MRI. Magnetic Resonance in Medicine, 2006, 56, 993-1000.	3.0	574
188	Comparative study into the robustness of compartmental modeling and model-free analysis in DCE-MRI studies. Journal of Magnetic Resonance Imaging, 2006, 23, 554-563.	3.4	145
189	Non-invasive mapping of corticofugal fibres from multiple motor areas—relevance to stroke recovery. Brain, 2006, 129, 1844-1858.	7.6	218
190	Blockade of Platelet-Derived Growth Factor Receptor-Beta by CDP860, a Humanized, PEGylated di-Fab', Leads to Fluid Accumulation and Is Associated With Increased Tumor Vascularized Volume. Journal of Clinical Oncology, 2005, 23, 973-981.	1.6	167
191	Optic radiation changes after optic neuritis detected by tractography-based group mapping. Human Brain Mapping, 2005, 25, 308-316.	3.6	114
192	Improved quantitative dynamic regional oxygen-enhanced pulmonary imaging using image registration. Magnetic Resonance in Medicine, 2005, 54, 464-469.	3.0	43
193	Probabilistic anatomical connectivity derived from the microscopic persistent angular structure of cerebral tissue. Philosophical Transactions of the Royal Society B: Biological Sciences, 2005, 360, 893-902.	4.0	312
194	Tracer Kinetic Modelling for T1-Weighted DCE-MRI. , 2005, , 81-92.		41
195	MR tractography predicts visual field defects following temporal lobe resection. Neurology, 2005, 65, 596-599.	1.1	117
196	Lateralization of ventral and dorsal auditory-language pathways in the human brain. NeuroImage, 2005, 24, 656-666.	4.2	458
197	Tracer Kinetic Model-Driven Registration for Dynamic Contrast Enhanced MRI Time Series. Lecture Notes in Computer Science, 2005, 8, 91-98.	1.3	11
198	Measuring Contrast Agent Concentration in T1-Weighted Dynamic Contrast-Enhanced MRI. , 2005, , 69-79.		40

#	Article	IF	CITATIONS
199	Is volume transfer coefficient (K(trans)) related to histologic grade in human gliomas?. American Journal of Neuroradiology, 2005, 26, 2455-65.	2.4	109
200	Comparative study of methods for determining vascular permeability and blood volume in human gliomas. Journal of Magnetic Resonance Imaging, 2004, 20, 748-757.	3.4	90
201	Analysis of MR diffusion weighted images. British Journal of Radiology, 2004, 77, S176-S185.	2.2	46
202	Prostate Cancer: Evaluation of Vascular Characteristics with Dynamic Contrast-enhanced T1-weighted MR Imaging—Initial Experience. Radiology, 2004, 233, 709-715.	7.3	204
203	Characterizing function–structure relationships in the human visual system with functional MRI and diffusion tensor imaging. NeuroImage, 2004, 21, 1452-1463.	4.2	149
204	Noninvasive in vivo demonstration of the connections of the human parahippocampal gyrus. NeuroImage, 2004, 22, 740-747.	4.2	116
205	Improved Regional Analysis of Oxygen-Enhanced Lung MR Imaging Using Image Registration. Lecture Notes in Computer Science, 2004, , 862-869.	1.3	0
206	A framework for a streamline-based probabilistic index of connectivity (PICo) using a structural interpretation of MRI diffusion measurements. Journal of Magnetic Resonance Imaging, 2003, 18, 242-254.	3.4	482
207	Application of a B-spline active surface technique to the measurement of cervical cord volume in multiple sclerosis from three-dimensional MR images. Journal of Magnetic Resonance Imaging, 2003, 18, 368-371.	3.4	23
208	From diffusion tractography to quantitative white matter tract measures: a reproducibility study. NeuroImage, 2003, 18, 348-359.	4.2	219
209	Combined functional MRI and tractography to demonstrate the connectivity of the human primary motor cortex in vivo. NeuroImage, 2003, 19, 1349-1360.	4.2	319
210	Diffusion tractography based group mapping of major white-matter pathways in the human brain. NeuroImage, 2003, 19, 1545-1555.	4.2	116
211	The longitudinal relation between brain lesion load and atrophy in multiple sclerosis: a 14 year follow up study. Journal of Neurology, Neurosurgery and Psychiatry, 2003, 74, 1551-1554.	1.9	81
212	Probabilistic Monte Carlo Based Mapping of Cerebral Connections Utilising Whole-Brain Crossing Fibre Information. Lecture Notes in Computer Science, 2003, 18, 684-695.	1.3	174
213	Three-dimensional modeling of perpendicular reading with a soft underlayer. Journal of Applied Physics, 2002, 91, 8366.	2.5	22
214	T1 histograms of normal-appearing brain tissue are abnormal in early relapsing-remitting multiple sclerosis. Multiple Sclerosis Journal, 2002, 8, 211-216.	3.0	36
215	Quantitative 1H MRS imaging 14 years after presenting with a clinically isolated syndrome suggestive of multiple sclerosis. Multiple Sclerosis Journal, 2002, 8, 207-210.	3.0	62
216	Measurement of atrophy in multiple sclerosis: pathological basis, methodological aspects and clinical relevance. Brain, 2002, 125, 1676-1695.	7.6	534

#	Article	IF	CITATIONS
217	Brain atrophy in clinically early relapsing–remitting multiple sclerosis. Brain, 2002, 125, 327-337.	7.6	417
218	Estimating distributed anatomical connectivity using fast marching methods and diffusion tensor imaging. IEEE Transactions on Medical Imaging, 2002, 21, 505-512.	8.9	270
219	Initial Demonstration of in Vivo Tracing of Axonal Projections in the Macaque Brain and Comparison with the Human Brain Using Diffusion Tensor Imaging and Fast Marching Tractography. NeuroImage, 2002, 15, 797-809.	4.2	171
220	Investigating Cervical Spinal Cord Structure Using Axial Diffusion Tensor Imaging. NeuroImage, 2002, 16, 93-102.	4.2	240
221	Exploring white matter tracts in band heterotopia using diffusion tractography. Annals of Neurology, 2002, 52, 327-334.	5.3	55
222	Reproducibility of in vivo metabolite quantification with proton magnetic resonance spectroscopic imaging. Journal of Magnetic Resonance Imaging, 2002, 15, 219-225.	3.4	43
223	The reproducibility and sensitivity of brain tissue volume measurements derived from an SPMâ€based segmentation methodology. Journal of Magnetic Resonance Imaging, 2002, 15, 259-267.	3.4	136
224	ADC mapping of the human optic nerve: Increased resolution, coverage, and reliability with CSF-suppressed ZOOM-EPI. Magnetic Resonance in Medicine, 2002, 47, 24-31.	3.0	129
225	MRI measurement of blood-brain barrier permeability following spontaneous reperfusion in the starch microsphere model of ischemia. Magnetic Resonance Imaging, 2002, 20, 221-230.	1.8	44
226	The relationship between lesion and normal appearing brain tissue abnormalities in early relapsing remitting multiple sclerosis. Journal of Neurology, 2002, 249, 193-199.	3.6	64
227	In vivo tracing of anatomical fibre tracts in the Macaque monkey brain by diffusion tensor imaging (DTI). NeuroImage, 2001, 13, 258.	4.2	1
228	Preliminary evidence for neuronal damage in cortical grey matter and normal appearing white matter in short duration relapsing-remitting multiple sclerosis: a quantitative MR spectroscopic imaging study. Journal of Neurology, 2001, 248, 131-138.	3.6	136
229	Accurate multislice gradient echoT1 measurement in the presence of non-ideal RF pulse shape and RF field nonuniformity. Magnetic Resonance in Medicine, 2001, 45, 838-845.	3.0	101
230	Effects of Androgen Deprivation on Prostatic Morphology and Vascular Permeability Evaluated with MR Imaging. Radiology, 2001, 218, 365-374.	7.3	143
231	Distributed Anatomical Brain Connectivity Derived from Diffusion Tensor Imaging. Lecture Notes in Computer Science, 2001, , 106-120.	1.3	16
232	Nonlinear smoothing for reduction of systematic and random errors in diffusion tensor imaging. Journal of Magnetic Resonance Imaging, 2000, 11, 702-710.	3.4	116
233	A 1H magnetic resonance spectroscopy study of aging in parietal white matter: implications for trials in multiple sclerosis. Magnetic Resonance Imaging, 2000, 18, 455-459.	1.8	71
234	Magnetic resonance imaging screening in women at genetic risk of breast cancer: imaging and analysis protocol for the UK multicentre study. Magnetic Resonance Imaging, 2000, 18, 765-776.	1.8	104

#	Article	IF	CITATIONS
235	Improving image quality and T1 measurements using saturation recovery turboFLASH with an approximate K-space normalisation filter. Magnetic Resonance Imaging, 2000, 18, 157-167.	1.8	40
236	In vivo 1 H-magnetic resonance spectroscopy of the spinal cord in humans. Neuroradiology, 2000, 42, 515-517.	2.2	41
237	Diffusion tensor imaging demonstrates deviation of fibres in normal appearing white matter adjacent to a brain tumour. Journal of Neurology, Neurosurgery and Psychiatry, 2000, 68, 501-503.	1.9	116
238	Dynamic Contrast Enhanced MRI of Prostate Cancer: Correlation with Morphology and Tumour Stage, Histological Grade and PSA. Clinical Radiology, 2000, 55, 99-109.	1.1	320
239	Variations in T1 and T2 relaxation times of normal appearing white matter and lesions in multiple sclerosis. Journal of the Neurological Sciences, 2000, 178, 81-87.	0.6	114
240	MTR and T1 provide complementary information in MS NAWM, but not in lesions. Multiple Sclerosis Journal, 2000, 6, 327-331.	3.0	1
241	Wallerian Degeneration in the Optic Radiation After Temporal Lobectomy Demonstrated In Vivo with Diffusion Tensor Imaging. Epilepsia, 1999, 40, 1155-1158.	5.1	49
242	1 H Magnetic resonance spectroscopy of normal appearing white matter in primary progressive multiple sclerosis. Journal of Neurology, 1999, 246, 1023-1026.	3.6	130
243	Short echo time single-voxel1H magnetic resonance spectroscopy in magnetic resonance imaging-negative temporal lobe epilepsy: Different biochemical profile compared with hippocampal sclerosis. Annals of Neurology, 1999, 45, 369-376.	5.3	131
244	Estimating kinetic parameters from dynamic contrast-enhanced t1-weighted MRI of a diffusable tracer: Standardized quantities and symbols. Journal of Magnetic Resonance Imaging, 1999, 10, 223-232.	3.4	2,856
245	A Direct Demonstration of both Structure and Function in the Visual System: Combining Diffusion Tensor Imaging with Functional Magnetic Resonance Imaging. NeuroImage, 1999, 9, 352-361.	4.2	84
246	Proton MR spectroscopy in clinically isolated syndromes suggestive of multiple sclerosis. Journal of the Neurological Sciences, 1999, 166, 16-22.	0.6	90
247	Pharmacokinetic Analysis of Neoplasms Using Contrast- enhance^ Dynamic Magnetic Resonance Imaging. Topics in Magnetic Resonance Imaging, 1999, 10, 130-142.	1.2	50
248	Nonlinear Smoothing of MR Images Using Approximate Entropy — A Local Measure of Signal Intensity Irregularity. Lecture Notes in Computer Science, 1999, , 484-489.	1.3	4
249	Spinal cord atrophy and disability in MS. Neurology, 1998, 51, 234-238.	1.1	217
250	The structural and functional mechanisms of motor recovery: complementary use of diffusion tensor and functional magnetic resonance imaging in a traumatic injury of the internal capsule. Journal of Neurology, Neurosurgery and Psychiatry, 1998, 65, 863-869.	1.9	110
251	Probing tumor microvascularity by measurement, analysis and display of contrast agent uptake kinetics. Journal of Magnetic Resonance Imaging, 1997, 7, 564-574.	3.4	191

A level sets approach to determining brain region connectivity. , 0, , .

#	Article	IF	CITATIONS
253	Detection and classification of MS using magnetisation transfer ratio images. , 0, , .		0
254	T1-W DCE-MRI:T1-Weighted Dynamic Contrast-Enhanced MRI. , 0, , 341-364.		24
255	Volume and Atrophy. , 0, , 533-558.		2
256	MR perfusion imaging in oncology: applications outside the brain. , 0, , 238-254.		0
257	Estimating kinetic parameters from dynamic contrast-enhanced t1-weighted MRI of a diffusable tracer: Standardized quantities and symbols. , 0, .		11